Closed Loop IBC Results from Recent CH-53G Flight Tests

Uwe T.P. Arnold, Director R&D, uwe.arnold@zf.com
Daniel Fürst, Project Manager, daniel.fuerst@zf.com
ZF Luftfahrttechnik GmbH, Calden/Germany

Abstract

Since December 2001, ZF Luftfahrttechnik GmbH (ZFL) has conducted open and closed loop IBC (Individual Blade Control) flight tests with the CH-53G IBC testbed of the German Federal Armed Forces Engineering Center for Aircraft. Over 25 flight hours had been spent in an “open loop” campaign to investigate the positive IBC effects. Early during the flight tests, it became clear that the response of the aircraft to the IBC inputs exceeded the initial expectations.

During the past two years, ZFL has expanded the open loop IBC system to enable a closed loop operation for automatic online optimization of the required IBC inputs. The controller design was performed under Matlab/Simulink and automatically implemented on a dSPACE real-time system. The closed loop control system added to the open loop core system extends the existing cascade control structure by an outer control loop. This outer control loop was used to implement different control tasks which were then investigated during the closed loop campaign. The main focus was put on vibration reduction in the fuselage. Further tests have addressed the load reduction potential of IBC. The capabilities of IBC were demonstrated for different single- and multiple-harmonic inputs in different steady and maneuvering flight conditions at different forward speeds. The predicted improvements through the application of more than one frequency could clearly be shown.

Different cost functions have been investigated with the controller using single or multiple sensor signals. It turned out that even simple cost functions based on only few sensor signals were practical since often also the not included sensor locations clearly benefited from that particular input. The amplitudes applied by the controller were in the order of 0.1 to 0.5deg which has underlined the effectiveness of even small blade pitch inputs.

The paper gives a brief overview of the architecture of the closed loop system and the implemented control strategies. The main focus is put on the test results gathered during the different closed loop flights. Beside the beneficial vibration reduction also some other IBC effects are discussed.

Notation

AccHGx, -y, -z	g	acceleration at main gearbox in x-, y-, z-direction
AccHeckx, -y, -z	g	acceleration at tail rotor gearbox in x-, y-, z-direction
AccLadx, -y, -z	g	acceleration at cargo compartment in x-, y-, z-direction
AccPilx, -y, -z	g	acceleration close to pilot seat in x-, y-, z-direction
A_n	deg	n/rev component IBC amplitude (AMPLn in figures)
CLCS		Closed Loop Control System
g	m/s^2	9.81, gravity constant
HHC		Higher Harmonic Control
IBC		Individual Blade Control
J_{ctrl}	-	cost function to be minimized
J	-/g/N	square root of cost function J without weighting of IBC-inputs and IBC-input changes
MTOW		Max. Take-Off Weight
N		6, number of blades
PLL		Pitch link load (=actuator axial force)
T	g/deg N/deg	IBC to output response transfer matrix (linear and quasi-static)
$T_{s,ctrl}$	s	controller sample time
VIAS	kts	Indicated Air Speed
W_i		weighting matrix w. respect to i
z	g	vector of vibrations and control loads (cos, sin component)
$e_{x,cos}$, $e_{x,sin}$	g	estimation error of cosine and sine component of x
$\vartheta_{IBC}=\Sigma A_n \cos(n\psi-\varphi_n)$		nominal pitch angle due to IBC
ϑ	deg	vector of higher harmonic IBC control inputs (cos, sin, compon.)
φ_n	deg	n/rev IBC control phase angle (PHASEn in figures)
Ω	rad/s	rotor rotational frequency

Presented at the 30th European Rotorcraft Forum,
14 – 16 September 2004, Marseilles, France

1 Introduction and Motivation

To extend the bandwidth of present primary control systems to the frequency range that affects blade motions, vibrations, and the local lift distribution, several active rotor control systems (HHC, IBC, etc.) of different architecture have been investigated in the past. Most of the HHC and IBC projects have been limited to wind tunnel tests in full scale, [4], [6], [14], or with MACH scaled models, [2], [16], [23]. During the last two decades HHC and later IBC systems have also been tested in flight, see [1], [3], [6], [12], [13], [19], [20], [22], [23], and [24]. Main focus of these test campaigns usually was to reduce cabin vibrations and/or BVI noise. Since HHC is limited to (N-1), N, and (N+1)/rev blade pitch inputs, HHC was found to show some deficiencies in reducing vibrations and BVI noise simultaneously for helicopters with more than three rotor blades. In spite of its technical complexity, IBC gained more and more interest by manufactures and operators alike. Reasons for this are also the additional applications like reduction of rotor power consumption in high speed flight, control load reduction, etc., see [19], [20]. Both applications primarily rely on 2/rev inputs and therefore can not be realized by HHC systems.

ZFL has been partner within many of these IBC test programs and has designed, manufactured, certified, and tested a whole family of IBC systems using hydraulic blade root IBC actuators. Remarkable applications have been a flight worthy system used on Eurocopter's BO-105 S1 testbed, [7], [24], as well as two experimental systems used for full scale wind tunnel tests of BO-105 and UH-60 rotors at NASA Ames, [4], [11].

Based on the success of these programs ZFL was awarded a contract from the German Federal Office of Defense, Technology, and Procurement (BWB) to design, manufacture, install, qualify and flight test an open loop IBC system for the medium weight transport helicopter CH-53G. **Figure 1** shows a sketch of the IBC system integration into the CH-53G testbed.

The German Army's fleet of more than 90 aircraft is in service for approximately 30 years and many of them are scheduled to fly for another 25 years. This provides the motivation to consider suitable upgrades that can help to improve the performance and to contain the growing operating and maintenance costs of these ageing aircraft. The primary fields addressed are therefore:

- Component fatigue and failure induced by high vibratory stress
- Unscheduled maintenance cost due to high vibration level
- CRTs of dynamical components determined by high (control system) loads
- Enabling of high TOW and/or high speed operation currently prohibited with regard to component life time constrains

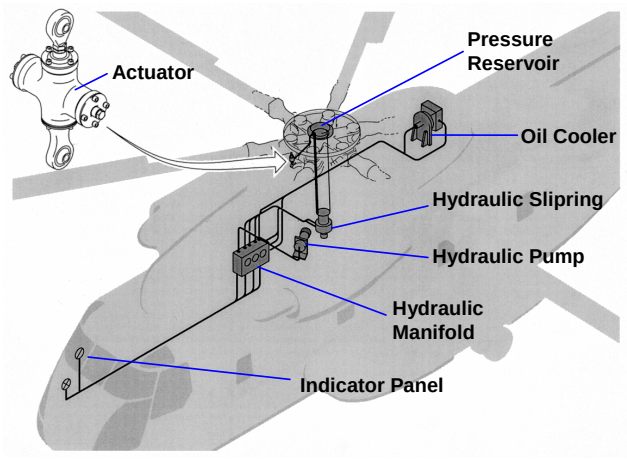

Figure 1: Principle lay-out of experimental IBC system installed in the CH-53G testbed

Other benefits that can be expected through the application of IBC include:

- Reduction of power required or improvement of equivalent lift-to-drag ratio at high forward speed
- Significant reduction in noise radiation
- Automated in-flight tracking

During the open loop project phase the IBC system had been extensively tested and operated for more than 70 hours. The following reductions were reached.

- vibrations at certain accelerometer stations by more than 90% in single axis or by about 60% in all spatial directions
- BVI noise in descent by 3dB
- power required at 130kts by 6%
- pitch link loads at 130kts by 30%,

see [19], [20] for details. These results have been achieved by using single harmonic IBC inputs of only 0.67° at a maximum and without ever optimizing the IBC amplitudes and phases explicitly. In open loop mode, systematic predefined sets of IBC-inputs were manually activated by the flight test engineer.

First IBC closed loop flight tests have been performed by Eurocopter, see [24], using a BO-105 helicopter fitted with an IBC system provided by ZFL. These first IBC closed loop test were aimed at noise reduction in descent flight and showed a reduction by 5dB through 2/rev IBC inputs of 1deg amplitude.

Based on the excellent open loop results ZFL was awarded a follow-on contract to extend and flight test the existing IBC system of the CH-53G in closed loop mode. For details of the project history and a comprehensive description of the hydraulic and electronic hardware see [9], [13], [19], [20], and [25].

2 Closed Loop IBC System

2.1 Control System Architecture

The IBC open loop core system with its safety features has almost completely been retained for the closed loop campaign. To realize closed loop operation with regard to different goals the IBC system has been complemented by a separate closed loop control system (CLCS), which extends the cascade control structure of the open loop system by an outer control loop, see **Figure 2**. The outer control loop is used to realize the different control tasks to be investigated within the closed loop campaign, e.g. the reduction of vibrations and/or control.

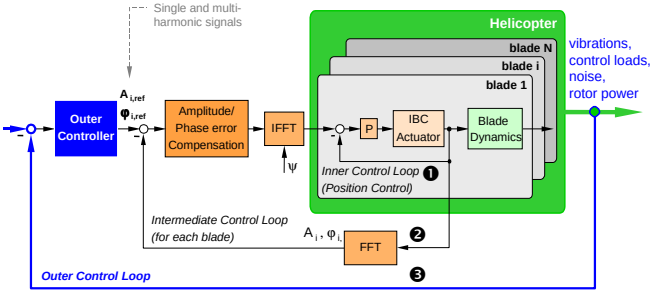

Figure 2: Cascade control structure of closed loop IBC system (1+2 = open loop; 1+2+3 = closed loop)

Figure 3 shows the hardware layout of the CLCS (left hand) and the interfaces used to merge the CLCS and the open loop IBC System (right hand) to the overall closed loop IBC control system. The CLCS consists of an industrial personal computer (IPC), a 12 inch touch screen display used as man-machine-interface (MMI) and a modular dSPACE real-time hardware system integrated in the IPC. The IPC runs a WindowsNT 4.0 operating system and is used as host to provide the experiment environment including all user interface and data storage capabilities. The modular dSPACE real-time hardware performs the real-time calculation of the closed loop algorithms. It provides the computing power and comprises a multi-I/O board and a serial interface board. The host interface for data exchange between the processor board and the host PC is implemented via ISA bus and communication between the processor board and the I/O boards are implemented via a peripheral high-speed I/O bus (PHS-bus). The communication of the CLCS and the IBC Open loop control system is realized by different analog and digital interfaces.

The model based controller design was performed under Matlab/Simulink. The controller has been implemented automatically on the dSPACE real-time system from block diagram level using the dSPACE Real-Time Interface (RTI).

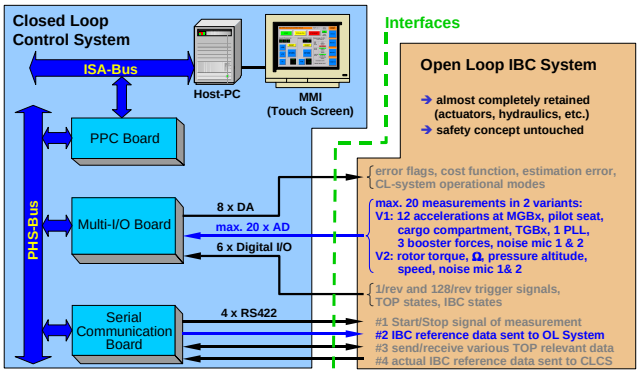

Figure 3: Complementation of the IBC control hardware by the new Closed Loop Control System

The closed loop algorithms are partitioned into seven tasks or subsystems which all together build up a Simulink library named "Adaptive Frequency Domain Controller Library". Due to this software architecture it has easily been possible to test the individual software tasks in offline and real-time simulations before the overall controller model has been built up. The most fundamental tasks are the System Identification Task, the Controller Task, the DFT task and the Task Handling and Command Generation Task.

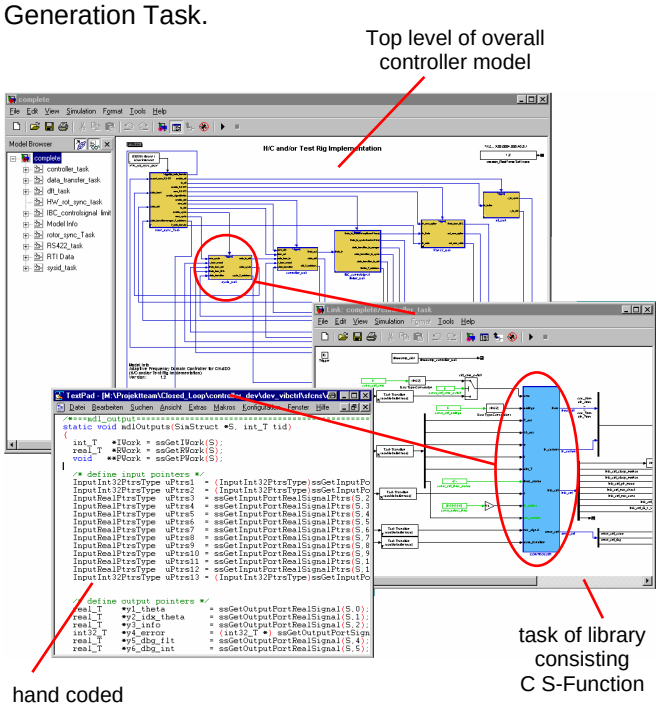

Figure 4: Structure of the implemented closed loop real-time software

Due to the complexity of the core algorithms of the tasks, e.g. the recursive system identification, these algorithms are implemented using hand coded C S-Functions. This is illustrated in **Figure 4**. The top level of the overall controller model comprises the tasks of the software library developed for this purpose.

Besides several Simulink blocks and subsystems which are used to realize the communication between the different tasks and to realize simple algorithms, each task consists of a hand coded C S-Function with the core algorithms implemented using finite state machines. The overall controller model is realized without timer tasks. The Task Handling and Command Generation Task, which represents the fastest task, is triggered by a hardware interrupt which is externally driven by a 128/rev signal. This trigger signal is generated within the IBC Open Loop System using a resolver signal and sent to the CLCS. Moreover, a 1/rev trigger signal is transmitted to the CLCS for synchronizing of all CLCS-tasks with the tasks implemented on the IBC Open Loop hardware. All other interrupt driven tasks on the CLCS are triggered by software interrupts generated within the Task Handling and Command Generation Task. The sample times of the Controller and System Identification Tasks can easily be modified by means of parameters in order to find out the optimum sample rates during flight tests. The results presented in this paper were conducted with a controller and system identification sample time $T_{s,ctrl}$ = 4rev, whereby the controller is updated only, if the IBC inputs of the last update step are cross-faded completely.

To control and monitor the closed loop test procedure during the flight tests an additional Man-Machine-Interface (MMI) was provided. It consists of a touch screen mounted adjacent to the retained open loop control panel in reach of the flight test engineer. Every closed loop trial is completely specified by a parameter set, which is generated prior to the flight. These parameter sets define the controlled variables and their individual weighting, the used IBC-frequencies, the controller and system identification algorithms, the initialization methods, the parameters of the algorithms, and the schedule of the corresponding experiment. Therefore, the flight test engineer only has to choose a parameter set and to start the corresponding test sequence.

For supervision of the closed loop flight trials from the ground based telemetry station an additional observation screen page had also been developed. By this screen it was possible to determine the current status of the closed loop control system. Moreover, the control performance and the used IBC inputs could be monitored online.

The modified IBC system is capable of generating single and mixed mode IBC inputs that consist of arbitrary combinations of all harmonics ranging from 2/rev – 7/rev. The highest control update rate provided by the open loop core system was 4/rev. Hence, the choice of the outer loop control was restricted to algorithms consistent with this specification.

2.2 Closed Loop Control Algorithms

The closed loop control algorithms used to form the outer control loop (**Figure 2**) for the vibration and control load reduction tasks are based on the well known frequency domain approach [8], [15-17]. The principle scheme of the adaptive controller is shown in **Figure 5**.

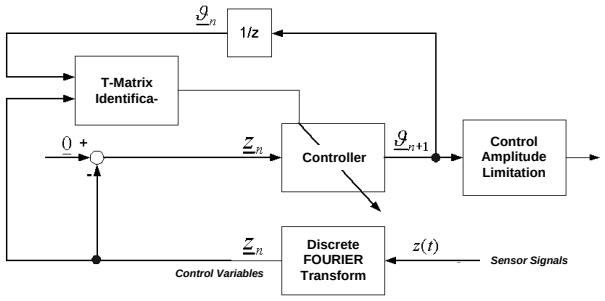

Figure 5: General representation of outer loop control algorithm

The frequency domain approach assumes a quasi-static linear relationship between the outputs z (harmonic components of measured vibrations and control loads) and the corresponding sets of IBC inputs ϑ. This relationship is modeled by the so-called linear T-matrix model [15-18]. The IBC inputs ϑ are characterized by the cosine and sine parts of the 2/rev – 7/rev components of the IBC-input. The output z is composed of the N/rev components of accelerations measured at different sensor locations (main gear box, pilot seat, cargo compartment and tail rotor gear box), the 2, 3 and 4/rev components from one pitch link load sensor as well as the N/rev components of the booster loads. This yields the following T-matrix model which is used for the controller synthesis:

$$z_n = z_{n-1} + T_n \left(\vartheta_n - \vartheta_{n-1}\right) \qquad (1)$$

where

$$z \in \mathbb{R}^{36},\ \vartheta \in \mathbb{R}^{12},\ T \in \mathbb{R}^{36,12}$$

and n denotes the current time step.

The overall outer control loop used for the vibration and control load reduction consists of two main tasks. A system identification task used to recursively estimate the linear T-matrix model (1), and a controller task used to calculate IBC inputs to accomplish the desired control task. The system identification can be performed using different Recursive Least Square methods (standard RLS, RLS with forgetting factor, stabilized RLS methods) or a Kalman filter based implementation. Both, local T-matrix model (1) and global T-matrix model [15] can be identified recursively within the implemented software. Below, only the recursive implementation of the Kalman filter based identification is given as an example:

$$n = 0;\ \text{initialize}\ \hat{T}_0^*, P_0$$

$$e_{n+1} = z_{n+1} - \hat{T}_n^*\,\vartheta_{n+1}^*$$

$$M_n = P_n + q\,I$$

$$k_{n+1}^T = \frac{\vartheta_{n+1}^{*T} M_n}{\vartheta_{n+1}^{*T} M_n\,\vartheta_{n+1}^* + r}$$

$$P_{n+1} = M_n\,(I - \vartheta_{n+1}^* k_{n+1})$$

$$\hat{T}_{n+1}^* = \hat{T}_n^* + e_{n+1} k_{n+1}^T$$

where

$$T_n^* := [T_n, z_{on}],\ \vartheta_n^* := [\vartheta^T, 1]^T \quad \text{(gobal model)}$$

$$T_n^* := [T_n],\quad \vartheta_n^* := [\vartheta] \quad \text{(local model)}$$

$$q, r \in \mathbb{R}^+$$

$$M_n, P_n \in \mathbb{R}^{13,13},\ k_n \in \mathbb{R}^{13} \quad \text{(gobal model)}$$

$$M_n, P_n \in \mathbb{R}^{12,12},\ k_n \in \mathbb{R}^{12} \quad \text{(local model)}$$

$$e_n \in \mathbb{R}^{36},\ k_n \in \mathbb{R}^{13},\ I \text{ as identity matrix}$$

and z_{on} represents the reference values of z without IBC and $\hat{x}$ is the estimate of x. The system identification task is capable to estimate the overall coupled MIMO (Multiple-Input-Muntiple-Output) T-matrix or sub-models only. If for example vibrations and control loads shall be addressed simultaneously, the impact of 2/rev IBC on the vibration components can be neglected in the identification algorithm. Using this feature it is possible to neglect small cross-coupling effects of IBC inputs in the controller design. Therefore, selected IBC frequencies can be used to control specified outputs.

Within the controller task the computation of IBC inputs is realized by solving the following optimization problem: minimize

$$J_{ctrl} = z_n^T W_z z_n + \vartheta_n^T W_\vartheta \vartheta_n + \Delta\vartheta_n^T W_{\Delta\vartheta} \Delta\vartheta_n \qquad (2)$$

with respect to the identified T-matrix model

$$z_n = z_{n-1} + \hat{T}_n\,(\vartheta_n - \vartheta_{n-1}) \qquad (3)$$

where

$$W_z = \text{diag}(w_{z1}, \ldots, w_{z36}) \in \mathbb{R}^{36,36},$$

$$W_\vartheta = \text{diag}(w_{\vartheta 1}, \ldots, w_{\vartheta 12}) \in \mathbb{R}^{12,12},$$

$$W_{\Delta\vartheta} = \text{diag}(w_{\Delta\vartheta 1}, \ldots, w_{\Delta\vartheta 12}) \in \mathbb{R}^{12,12},$$

$$\Delta\vartheta = \vartheta_n - \vartheta_{n-1}$$

The solution of the above optimization problem is either formulated using the feedback of measured values of z_n or using a feedback of identified reference values. For the feedback of z_n the control law results in

$$\vartheta_{n+1} = \left(D_n W_{\Delta\vartheta} + D_n \hat{T}_n^T W_z \hat{T}_n\right) \vartheta_n - \alpha D_n \hat{T}_n^T W_z z_n \qquad (4a)$$

with

$$D_n = \left(\hat{T}_n^T W_z \hat{T}_n + W_{\Delta\vartheta} + W_\vartheta\right)^{-1} \qquad (4b)$$

and

$$0 \le \alpha \le 1,\ D_n \in \mathbb{R}^{12,12}$$

The computation of equation (4) for the considered control task (e.g. minimize AccPilz using 5/rev IBC) is performed with a reduced set of system matrices and vectors to minimize the computational effort. This minimal set of rows and columns of the matrices and vectors necessary to compute the optimum IBC-inputs are chosen automatically according to the specification of the current control task. The configuration of the control task with all its parameters is realized by the mentioned parameter sets.

For the vibration reduction control task the IBC-frequencies 4 – 7/rev are preferred whereas 2/rev IBC is preferred for control system load reduction. Due to the various implementations of the system identification, the controller task and the possibility to tune these algorithms by various parameters using predefined data sets the outer control loop can represent the following structures:

- *non-adaptive closed loop:*
  no system identification during closed loop control and feedback of measured outputs (disturbances)
- *adaptive closed loop:*
  system identification during closed loop control and feedback of measured disturbances
- *non-adaptive feed forward:*
  no system identification during feed forward control and feed forward of identified reference values of disturbances
- *adaptive feed forward:*
  system identification during feed forward control and feed forward of identified reference values of disturbances

3 Closed Loop Flight Test Results

Until end of June 2004 more than 30 hours have been spent in flight testing the IBC system in closed loop configuration. Some 12 hours were devoted to certification issues whereas the rest was used to investigate the performance of the various control configurations. **Figure 6** gives an overview on the flight test conditions and corresponding IBC settings during those flights. Depending on the actual weather conditions the flight tests were conducted in altitudes ranging from 2500 to 6900ft. The aircraft weight was kept between 75% and 85% of the CH-53G's 42,000lbs MTOW.

	Flight Condition	IBC Inputs (max. Amplitudes)						
		2/rev	3/rev	4/rev	5/rev	6/rev	7/rev	Total Amplitude
Vibrations	40kts HF				0,25°			
	60kts HF			0.5°	0.4°	0.3°		0.7°
	130kts HF			0.5°	0.4°	0.3°	0.3	0.7°
	manoeuvre flights				0.4°			0.4°
Pitch Link Loads & Booster Loads	130 kts HF	1.1°						1.1°
Power Required	130 kts HF	1.1°						1.1°

Figure 6: Overview on flight test conditions of closed loop campaign

3.1 Vibration Reduction

The main focus of the closed loop flights was put on vibration reduction at different sensor locations and sensor axes in steady level flight at 70 and 130kts.

The reduction of vibrations is a well proven application for HHC and IBC. Since the vibrations in the non-rotating frame are of multiple integers of blade number N times rotor speed Ω, the introduction of (N-1)·Ω, N·Ω and (N+1)·Ω frequencies by HHC or IBC is known to be a powerful means in counteracting rotor induced vibrations. However, substantial wind tunnel tests using the four-bladed rotors of a BO105 and UH-60 have shown, that the frequency (N-2)·Ω has a considerable effect in reducing vibrations, too, [4] and [14]. Similarly, the open loop flight tests with the six-bladed CH-53G had shown, that 4/rev is a very useful for this particular rotor [13], [19], [20]. These frequencies are provided exclusively by IBC and can not be realized through HHC.

The time histories shown hereafter are all of similar structure. They are given in the following 2 by 2 arrangement for single-harmonic and 2 by 3 arrangement for multi-harmonic inputs with two IBC frequencies, respectively.

controller state (info_ctrl_state)	amplitudes of n/rev IBC input (AMPLn)	*amplitudes of m/rev IBC input (AMPLn)*
square root of cost function J (here: 6/rev vibration components)	phase angles of n/rev IBC input (PHASEn)	*phase angles of m/rev IBC input (PHASEn)*

The test procedure always started with a reference measurement (no IBC input) followed by an open loop phase sweep. The latter was used to identify the T-matrix of the plant for the closed loop sequence to follow. For the selected frequencies the IBC phase angle was varied in 60deg increments at a fixed IBC amplitude. This phase sweep was followed by a second reference measurement before the closed loop phase itself was started. Finally, each measurement was concluded by a third reference measurement. This procedure can be easily identified in the figures with help of the controller state info_ctrl_state:

- info_ctrl_state = 1 ➔ reference measurement
- info_ctrl_state = 2 ➔ open loop phase sweep
- info_ctrl_state = 3 ➔ closed loop operation

Note that due to the chosen IBC amplitudes, the vibrations in some cases become worse during the complete phase sweep when compared to the reference vibrations. This is explained by the observation that the optimum amplitudes computed by the controller during the closed loop operation are in most cases smaller than the fixed IBC amplitudes chosen for the phase sweep. It is well known, that using too large amplitudes even at the right phase angle can worsens the vibration level. The large amplitudes and the number of IBC phase points during the phase sweep were chosen to get significant excitations of the plant. To get comparable results every test point was performed using exactly the same test procedure. Moreover, all variables of the algorithms were initialized with identical values (e.g. the T-Matrix initialized as a zero matrix). In an applicable controller layout suitable initialization values from preceding flights could be stored. Thus, due to the continuing identification process in parallel to the closed loop operation, it might be possible to completely skip that explicit identification phase.

3.1.1 Single-Harmonic IBC at 70kts

From the open loop flight tests [13] it was known that even single mode IBC inputs with IBC-frequencies between 4 and 7/rev could considerably reduce the vibrations at certain sensor locations. Please note that the given vibration figures refer to the 6/rev (i.e. blade passage frequency) component only. This is justified by the fact that the vibration spectrum is clearly dominated by this very frequency, compare **Figure 7**.

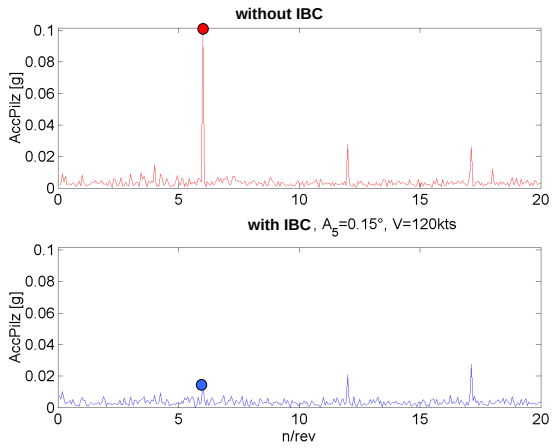

Figure 7: Effect of 5/rev IBC on z-vibration spectrum at pilot seat (from open loop flight test)

The diagrams of **Figure 8** through **Figure 12** show the effect of single harmonic IBC inputs on different cost functions. Due to the flexible implementation of the control algorithm it was possible to include arbitrary combinations of sensor signals in that cost function. For the conducted flight tests all elements within the cost function were weighted equally. For a later commercial application it might be worthwhile to consider a customized weighting by which the vibration reduction benefit is directed to the desired locations in the aircraft (e.g. passenger compartment for VIP transport or known week spots in the fuselage structure for maintenance cost reduction).

Figure 8 shows the effect of (N-2)·Ω (i.e. 4/rev) inputs on the 6/rev vertical vibrations at the pilot seat.

A reduction in the order of 70% is achieved with the controller commanding approximately 0.2deg of IBC amplitude.

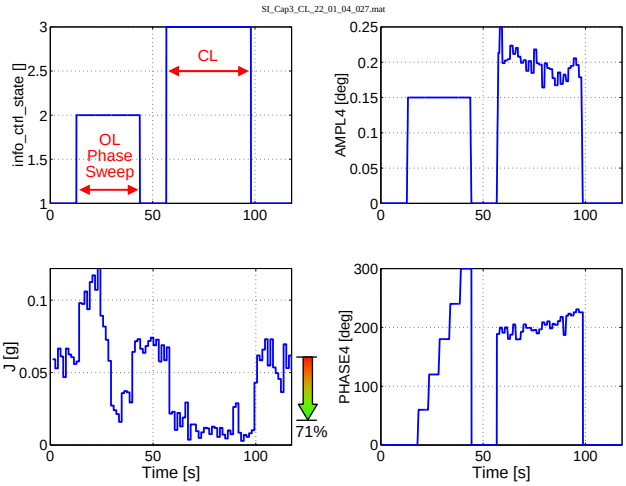

Figure 8: Closed loop control performance at 70kts, controlled variable: 6/rev AccPilz, 4/rev IBC

Using 5/rev inputs the reduction for the same cost function is even better and stays consistently beyond 90%, while the required amplitude fluctuates around 0.1deg, about half the value required with the 4/rev input, see **Figure 9**.

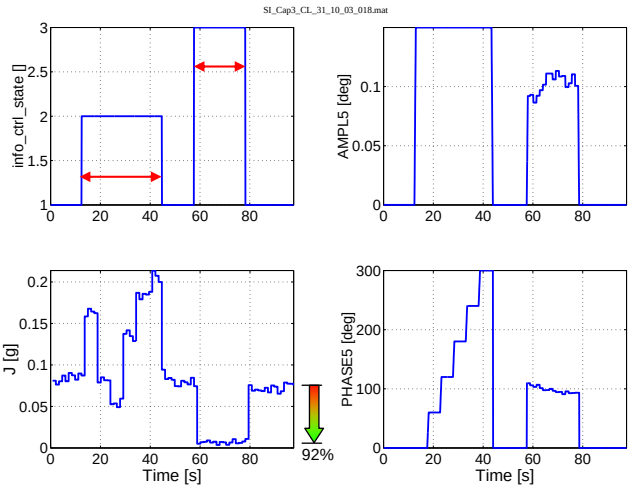

Figure 9: Closed loop control performance at 70kts, controlled variable: 6/rev-AccPilz, 5/rev IBC

Including only one of 12 measured vibratory components within the cost function could be quite daring, since one might risk to redistribute the vibrations to a non-controlled area of the aircraft. Therefore, **Figure 10** gives the time histories of all observed acceleration components (**Acc…**) throughout the helicopter (**…HG** = main gearbox, **…Pil** = pilot seat, **…Lad** = cargo compartment, **…Heck** = tail rotor gearbox) for the same test sequence.

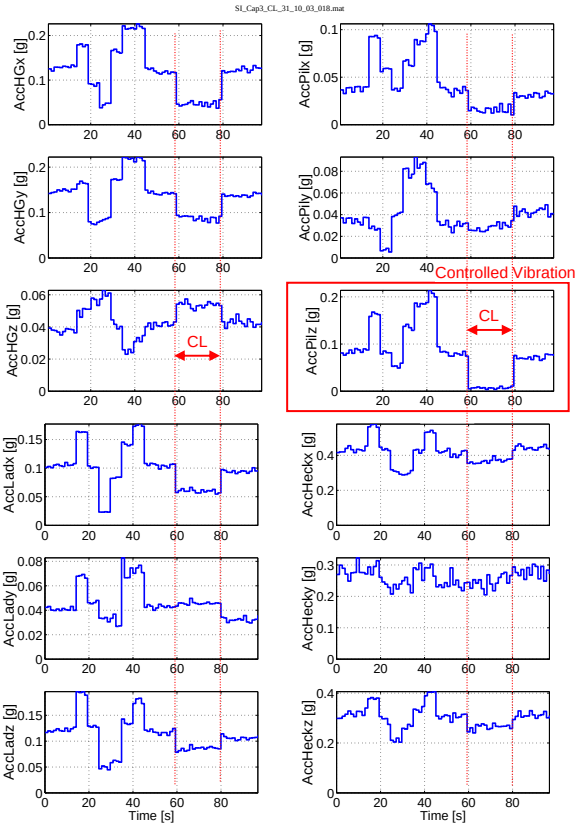

Figure 10: Closed loop control performance for all 12 accelerations at 70kts, controlled variable: 6/rev AccPilz, 5/rev IBC

Surprisingly, it turned out that most other locations also profited from this simple control loop and, interestingly enough, only the vertical component at the main gearbox was slightly increased. This indicates that concentrating on the vibrations at the rotor (or close to it) only might not automatically lead to an optimum vibratory condition in the fuselage. This is one reason, why ZFL favours the applied frequency domain approach instead of suppressing blade reaction forces at the individual blade roots in the rotating frame.

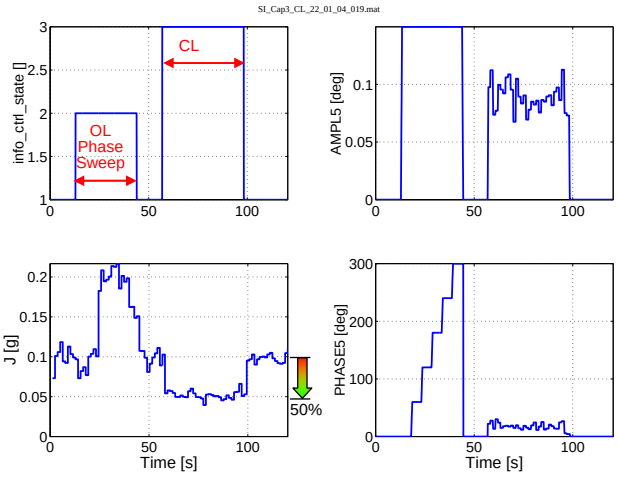

Figure 11: Closed loop control performance at 70kts, controlled variables: 6/rev AccHGy & AccPilz, 5/rev IBC

Nevertheless, step by step more vibratory components in different axes and from different locations were added to the cost function. Unless additional IBC frequencies were added, the reduction of the cost function values became somewhat smaller, while the positive effects were spread over a larger area of the aircraft. **Figure 11** and **Figure 12** give two corresponding examples. In these cases, 5/rev IBC had been used to simultaneously optimize two vibratory components (pilot seat and the main gearbox) or three vibratory components (main gearbox and 2x cargo compartment), respectively.

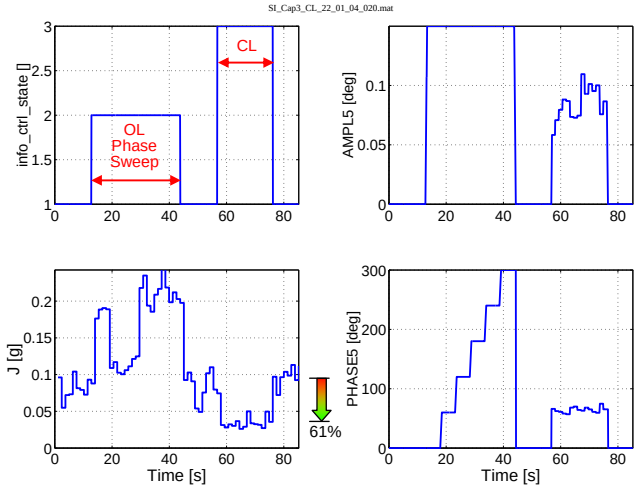

Figure 12: Closed loop control performance at 70kts, controlled variables: 6/rev AccHGx & AccLadx & AccLadz, 5/rev IBC

3.1.2 Multi-Harmonic IBC at 70kts

As shown in the previous section single harmonic IBC becomes less effective if one needs to reduce vibrations at many locations and multiple axes simultaneously. Therefore, already at the end of the open loop campaign identified T-matrix models (in a nonlinear version, see [10] and [13]) were used to predict optimum mixed mode inputs using 4 to 7/rev. In the following example the cost function consisted of the three equally weighted acceleration components x, y, z (corresponding to the local "spatial" vibrations) at the main gearbox or the pilot seat, respectively.

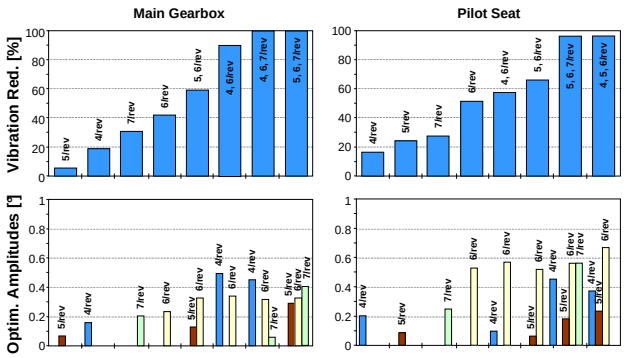

Figure 13: Predicted spatial vibration reduction at 120kts for main gearbox and pilot seat

Figure 13 shows the effect of different frequency combinations on the cost function as yielded by a numerical optimization based on open loop data.
As expected, applying more than one frequency considerably improves the reduction of the spatial vibrations. From this nonlinear extrapolation it was concluded that a mixture of three frequencies should be sufficient to almost completely cancel the spatial vibrations at any chosen location. And again, the useful contribution of (N-2)/rev IBC (4/rev in this case) was underlined. According to these calculations the over-all authority required for the vibration reduction seemed to stay below 1deg even in the multi-harmonic case. This was the motivation to continue the closed loop flight testing in multi-harmonic mode.

To validate these expectations the flight test point of **Figure 12** was repeated with two IBC frequencies (5 and 6/rev) enabled. The success can easily be seen in **Figure 14**. The positive IBC effect on the cost function during the closed loop phase increases from about 60% to more than 80%. The required authority for both frequency contributions combined reaches +/-0.25deg in this case.

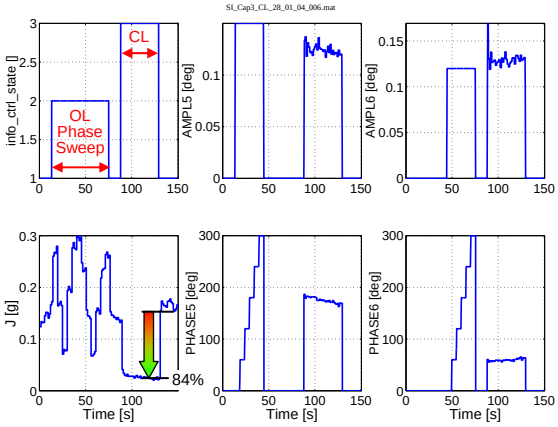

Figure 14: Closed loop control performance at 70kts, controlled variables: 6/rev AccHGx & AccLadx & AccLadz, 5 & 6/rev IBC

A similar example is given in **Figure 15**, where all three spatial directions of the cargo compartment vibrations have been included in the cost function. In this case a combination of 4 and 6/rev IBC input has been used. Again, as in the single harmonic case (**Figure 8** vs. **Figure 9**), the usage of 4/rev increases the required amplitudes. Because the maximum amplitudes were still restricted in that certification stage of the test program (these software-imposed limits were lifted shortly thereafter), the controller ran into saturation for both frequencies. Consequently, the performance with respect to the vibration reduction was visibly degraded. But again, the controller did command a considerable portion of 4/rev input, which would not be expected from linear theory but shows the strong inter-harmonic coupling, see [19] for more detailed explanation.

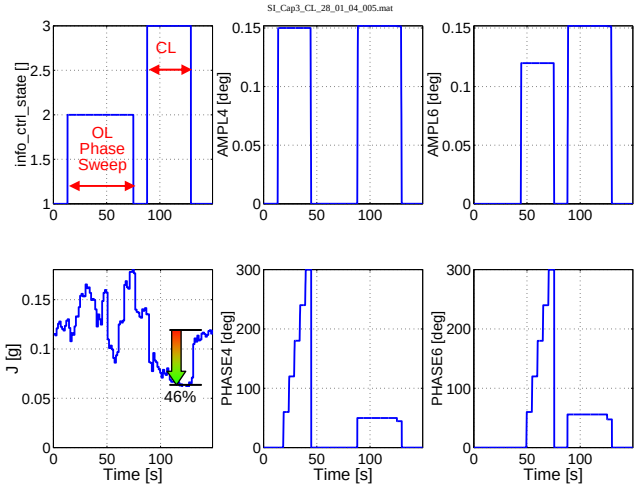

Figure 15: Closed loop control performance at 70kts, controlled variables: 6/rev AccLadx & AccLady & AccLadz, 4 & 6/rev IBC

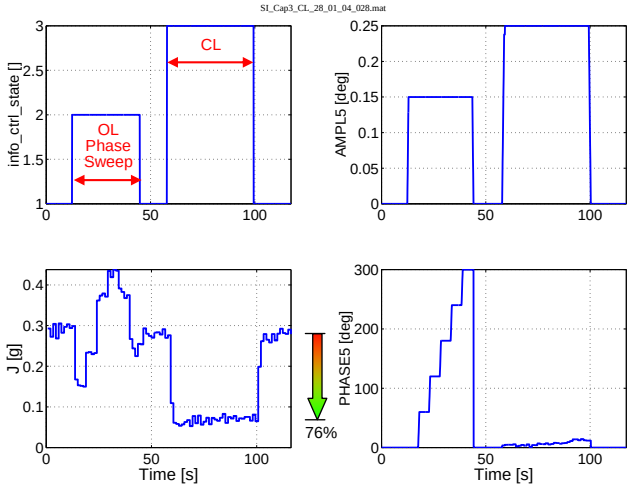

Figure 17: Closed loop control performance at 130kts, controlled variables: 6/rev AccHGy & AccPilz, 5/rev IBC

3.1.3 Single-Harmonic IBC at 130kts

The following diagrams show similar results from test flights at high forward speed. In the first example the vibration reduction at the pilot seat due to 5/rev inputs exceeds 80%, see **Figure 16**.

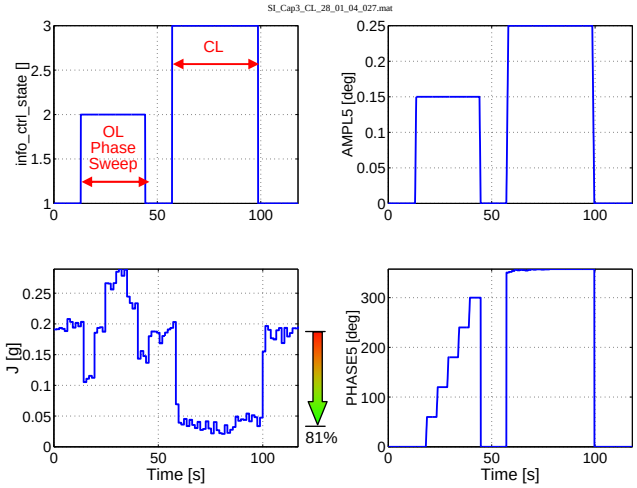

Figure 16: Closed loop control performance at 130kts, controlled variable: 6/rev AccPilz, 5/rev IBC

Here, the authority limit was reached even for this single harmonic case. Base on the already good reduction one should assume, however, that the optimum amplitude would have been only slightly higher. The inclusion of a second vibration component (y-axis at main gearbox) has almost no negative effect on the cost function during closed loop operation, see **Figure 17**.

With three components evaluated in the cost function, see **Figure 18**, the reduction still reaches almost 60%, which is well in line with the results at 70kts presented above (compare e.g. **Figure 12**). In this case the amplitude limitation of 0.25deg was active for few seconds only indicating that the optimum values were close to that limit.

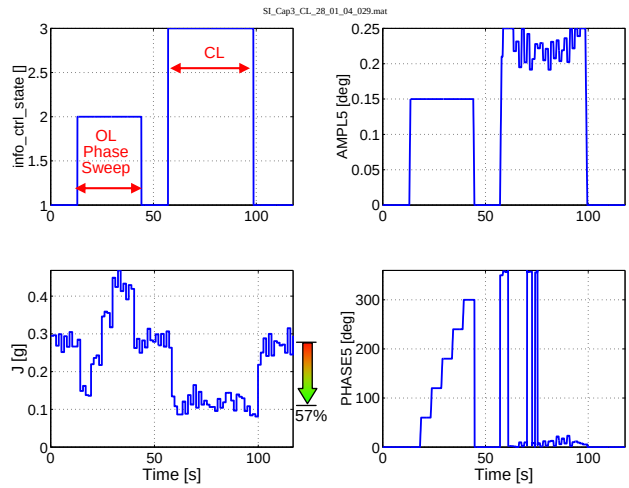

Figure 18: Closed loop control performance at 130kts, controlled variables: 6/rev AccHGx & AccPilz & AccLady, 5/rev IBC

The next two figures show again, how 4/rev can contribute to the vibration reduction. Although in both cases the controller run into saturation, still impressive and stable reductions were achieved for cost functions composed of two (**Figure 19**) or three (**Figure 20**) vibration components.

In general, the required amplitudes seem to increase with forward speed. Nevertheless, the results have confirmed that the amplitudes required for the CH-53G are smaller than those needed for the BO-105.

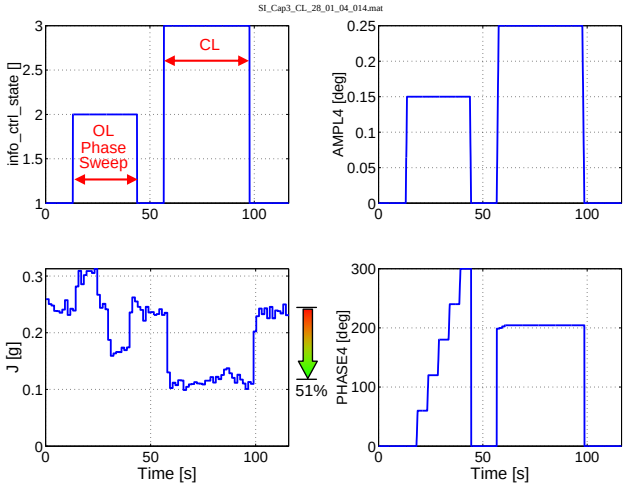

Figure 19: Closed loop control performance at 130kts, controlled variables: 6/rev AccHGy & AccPilz, 4/rev IBC

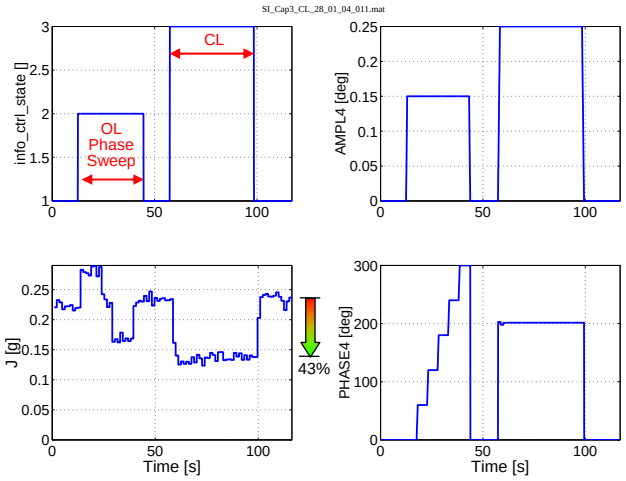

Figure 20: Closed loop control performance at 130kts, controlled variables: 6/rev AccPilx & AccPily & AccPilz, 4/rev IBC

3.1.4 Maneuvering Flights

All previously shown results correspond to steady horizontal flights, where disturbances were caused only by the atmospheric conditions and the pilot reactions to counteract them. Nevertheless, several of the presented diagrams clearly show that considerable changes of the amplitudes and phases were commanded from the controller to keep up with these small disturbances, compare e.g. **Figure 8** or **Figure 12**. Despite the fact that the bandwidth of the outer control loop was restricted by the dynamics of the inner loops of the retained open loop IBC system, the controller update rate (typically 1/4revs) seemed to be fast enough for those flight conditions. Now it had to be checked whether this would also hold for maneuvering flights. The following three figures show the IBC effect during a flight sequence with forward speed changing between 60 and 130kts, **Figure 21**, during a right/left turn sequence with 30deg bank angles, **Figure 22**, and during a descent flight ending in a typical flare, **Figure 23**.

For each case the upper two diagrams show the corresponding reference flights whereas the lower two give the closed loop IBC cases, respectively.

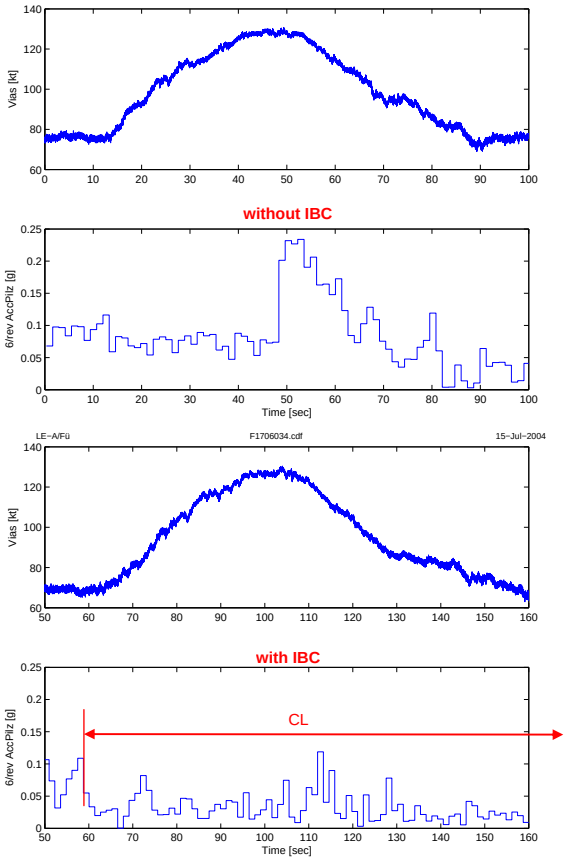

Figure 21: Forward speed and closed loop control performance during an acceleration und deceleration maneuver, controlled variable: 6/rev AccPilz, 5/rev IBC

In all three maneuvers the positive IBC effect can clearly be seen. In average the vibration levels were approximately halved. Moreover, the noticeable often sharp vibration rises during the most unsteady phases of the maneuvers are successfully suppressed, see especially the start of the deceleration in **Figure 21** and the flare in **Figure 23**. These results are very encouraging, since they show that there have never been situations in which IBC has increased the vibrations (e.g. due to lagging adaptation), a possibility which was discussed in [26] based on simulations with a linear model. Although the controller did vary the commanded IBC amplitudes by more than a factor of 3 and the IBC phase angles by up to 100deg in some situations, it does not seem to be necessary to speed up the refresh rates much further. This in turn would help to keep the frequency ranges of the rotor dynamics and the IBC control activity well separated, which prevents any stability issues to come into play. This property is confirmed by the fact that there was not one single test point during the whole flight test campaign where the pilot had to report that he felt any interactions between the controller adaptation and his trim activity.

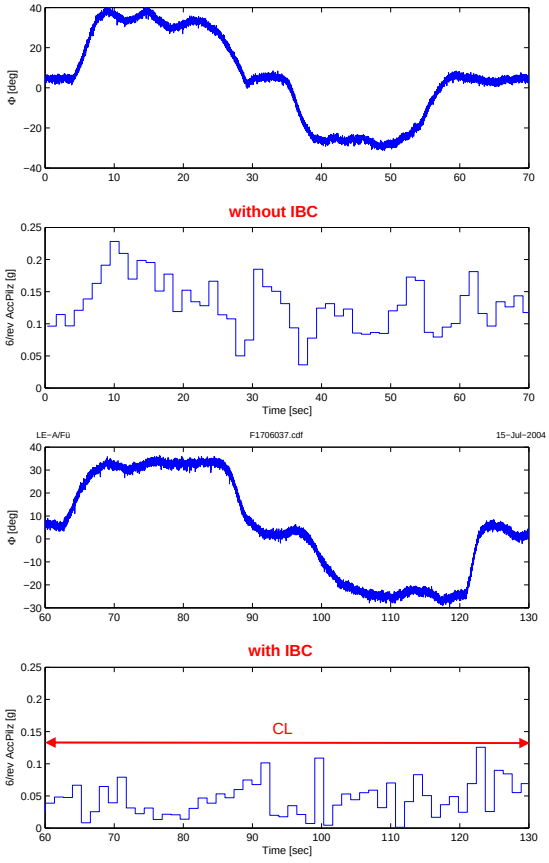

Figure 22: Closed loop control performance during a left and right turn maneuver at 70kts, controlled variable: 6/rev AccPilz, 5/rev IBC

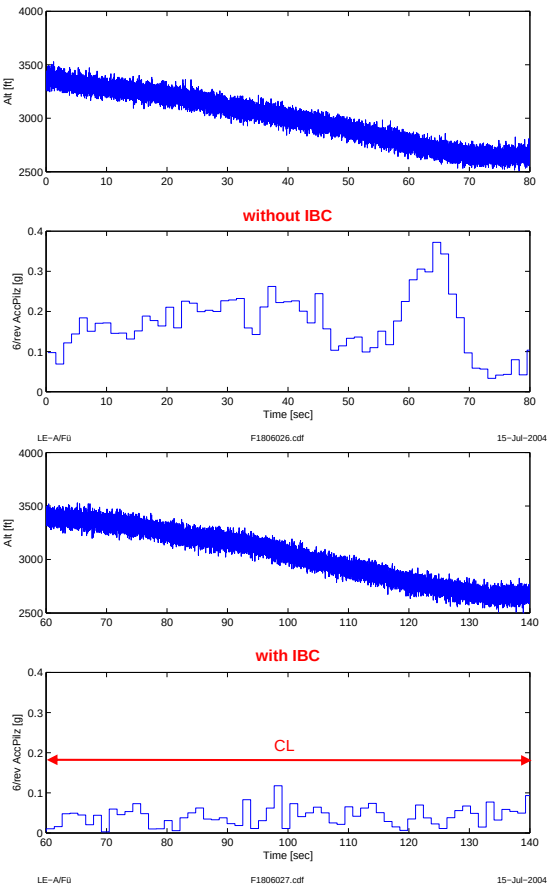

Figure 23: Closed loop control performance during a descent/flare maneuver at 50kts, controlled variable: 6/rev AccPilz, 5/rev IBC

3.2 Load Reduction

From the open loop tests it was known that high pitch link loads at high forward speed can effectively be reduced by application of suitable 2/rec IBC, see [19].

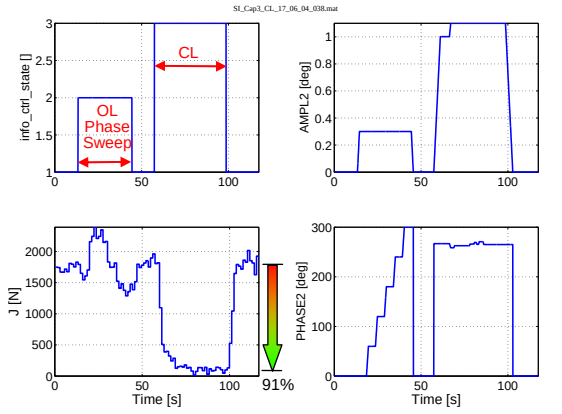

Figure 24: Closed loop control performance at 130kts, controlled variables: 2/rev-PLL, 2/rev IBC

This was successfully validated by the closed loop results. **Figure 24** shows the known test sequence, here with application of 2/rev inputs to reduce the 2/rev component of the pitch link loads (i.e. axial actuator forces). The cost function is impressively reduced to very small values within few seconds.

Since all of the first three higher harmonics 2/rev, 3/rev, and 4/rev contribute considerably to the pitch link load spectrum (beside the dominant 1/rev component) and 2/rev IBC shows an effect on all of them, see [19], the cost function was then modified to include (equally weighted) these three load components, **Figure 25**. Although the reduction of the cost function is clearly smaller compared to the preceding case, the positive effect on the peak-to-peak values of the time history is even slightly better.

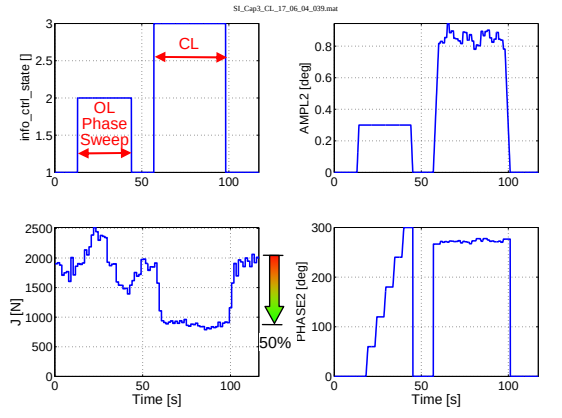

Figure 25: Closed loop control performance at 130kts, controlled variables: 2 & 3 & 4/rev PLL, 2/rev IBC

Figure 26 clearly shows this positive IBC effect on the pitch link load amplitudes. **Figure 27** directly compares the cases without and with IBC by showing averaged time histories plotted over one rotor revolution. It requires in the order of 0.9deg of 2/rev IBC to reduce the peak-to-peak values by nearly 30%. These results are in close accordance to the open loop results [20].

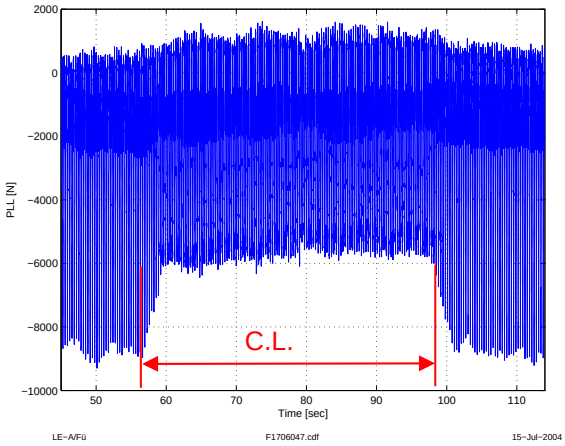

Figure 26: Closed loop control performance at 130kts, controlled variables: 2 & 3 & 4/rev PLL, 2/rev IBC

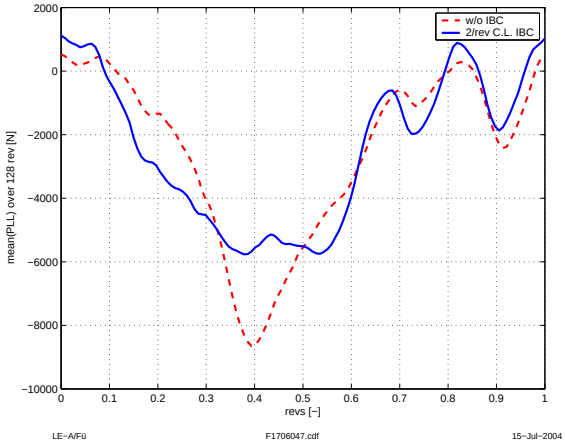

Figure 27: Comparison of averaged PLL time histories without and with 2/rev IBC at 130kts, controlled variables: 2 & 3 & 4/rev PLL

3.3 Controller Performance and Side Effects

It has already been mentioned that the commanded IBC amplitudes and phases sometimes change quite considerably during a test sequence. This is caused by the feedback of the changed vibrations as well by the adaptation of the T-matrix within the controller algorithm. **Figure 28** shows how the averaged commanded amplitude and phase values change from test point to test point. Although the test sequences were taken directly one after the other in the same flight condition (compare the forward speed in the lower diagram), the optimum values are noticeably drifting within this less than one-hour flight. This clearly indicates that an open loop system with any type of gain scheduling seems not to be feasible for an operational application.

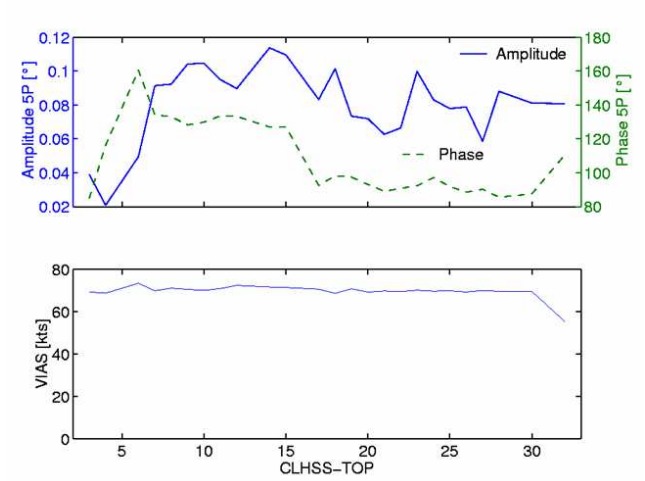

Figure 28: Optimum 5/rev amplitude and phase vs. test points for close to constant flight condition

Figure 29 shows in more detail (for the example of **Figure 16**) how fast the controller typically reduces the vibrations after it has been activated. Within two control steps (i.e. approximately 2.6 seconds) the reduced vibration level is reached. This comes close to the theoretical deadbeat property of the closed loop control system that could be expected if the following assumptions were always valid: $\alpha = 1$ in Eq. (4a) and the helicopter dynamics were perfectly modeled by the identified T-matrix.

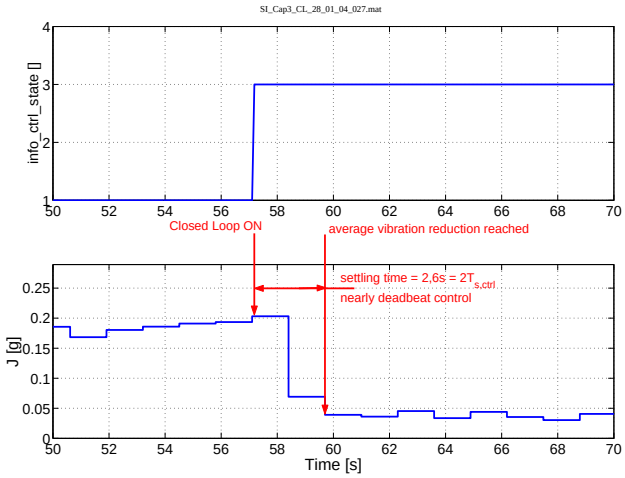

Figure 29: Illustration of the close to deadbeat property of the disturbance rejection; 130kts, controlled variable: 6/rev AccPilz, 5/rev IBC

For the same example **Figure 30** illustrates the development of the estimation error over time. As long as info_sysid_state equals two, the system identification process is active and the T-matrix is updated recursively. For the flight test results presented here, the identification process has always been started at the begin of the open loop phase sweep and kept

active during the rest of the sequence i.e. also through the closed loop control portion. The estimation error is shown as cosine (bottom left) and sine (bottom right) component.

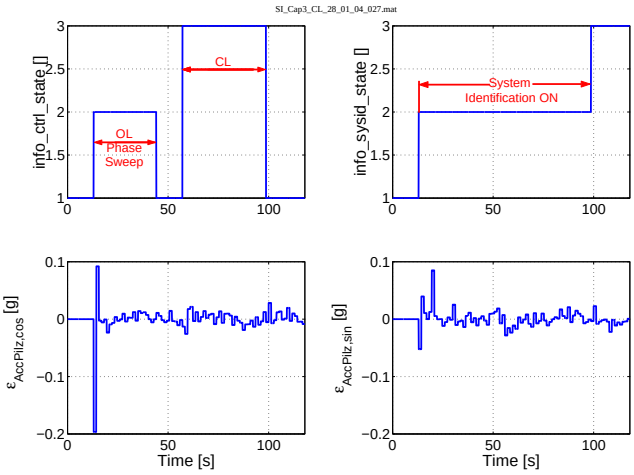

Figure 30: Estimation error time histories during test sequece;130kts, controlled variable: 6/rev AccPilz, 5/rev IBC

After the phase sweep and the system identification process have been started it takes only few seconds until the estimation error reaches very small values. It appears that less than the used six discrete phase angles are required to properly identify the T-matrix and hence the open loop sequence could be shortened considerably. As mentioned earlier, it might even be possible to completely skip that explicit phase sweep identification sequence by using appropriate start values for the T-matrix.

Obviously, introducing additional blade pitch motions can not only reduce but also increase control system loads. Therefore, during all flight tests the loads at the swashplate scissors and primary control boosters were continuously monitored. In most cases these loads were not significantly increased through the IBC inputs commanded by the controller. As an example **Figure 31** shows the impact of 4/rev IBC on the booster loads (corresponding to the case of **Figure 8**).

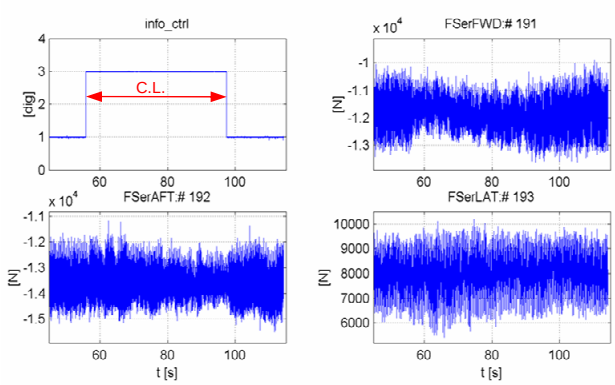

Figure 31: Impact of 4/rev IBC on booster loads at 70kts, controlled Variable: 6/rev AccPilz

While during closed loop operation the forward and aft servos saw somewhat smaller loads the lateral servo was loaded slightly higher, however well within its structural or hydraulic limits. In general, it can be stated that the higher the applied frequencies are the more dominant blade inertial effects become (in contrast to aerodynamic effects) and the higher the booster loads can rise for disadvantageous IBC settings. Therefore, using 4 through 6/rev for the vibration reduction task is clearly preferable to the HHC frequencies 5 through 7/rev. In any case, it seems to be always possible, to use the lower IBC frequencies at suitable amplitude/phase settings to positively alter the control system loads (compare section 3.2 and [20]) and thereby counteract the sporadic increase from the application of the higher IBC frequencies.

4 Conclusions and Outlook

The closed loop flight tests have confirmed the expectations derived from the open loop results. Moreover they have shown that automated IBC operation based on the described frequency domain closed loop approach is feasible. The following conclusions can be drawn:

- The chosen closed loop control algorithm is clearly capable of significantly reducing the vibrations in all investigated flight conditions
- Although the IBC amplitudes were limited by the software in some cases, no instabilities occurred. This clearly indicates the robustness of the closed loop system
- 4/rev IBC has been proven to efficiently contribute to the vibration reduction task
- Achieved vibration reductions in single mode were:
  - one controlled vibration component: up to 90%
  - two controlled vibration components: up to 75%
  - three controlled vibration components: up to 60%
- Mixed mode IBC inputs result in clearly improved vibration reduction compared to the corresponding single mode cases
  - two IBC frequencies, three controlled vibration components: up to 85%
- Although the number of vibration components being controlled was limited to three, the results clearly show a positive effect also on the non-controlled vibration components

Beside the IBC applications presented in this paper, additional valuable effects had been investigated in the preceding open loop campaign. These impressive findings comprise:

- 3dB BVI noise reduction during steady landing approach through 0.67deg 2/rev IBC
- Reduction of rotor power required at high forward speed by more than 6% also using 0.67 deg 2/rev IBC

see [19] and [20] for more details. One primary advantage of the IBC concept is that different deficiencies of a helicopter rotor operating in tangential flow can be addressed by one single system. In many cases it seems to be possible to pursue the different goals simultaneously (vibration reduction plus increased rotor efficiency plus reduced control system loads). This applies especially to the six-bladed CH-53G where the "vibration frequencies" (4 through 7/rev) and the "power and noise frequencies (2 and 3/rev) are well separated. Moreover, some of the goals do not interfere at all (e.g. noise reduction in maneuvers close to the ground versus power reduction at high speed level flight). In other cases it might also be helpful to define alternative cost functions which emphasize different goals and which can be chosen according to the respective mission (e.g. VIP comfort due to low cabin vibrations versus stress alleviation for lower maintenance cost).

Finally, it is obvious that an IBC retrofit kit will have to be optimized with respect to weight, cost and installation effort compared to the used experimental system. The latter was primarily designed to be an experimental tool for maximum flexibility and minimum interference with the testbed. The design goals for a production version are low weight, low power consumption, and small installation space as well as reliable function and autonomous operation. ZFL has pursued several design studies for different helicopters, not only by varying the details of the mechanical solution but also under consideration of alternative methods for the power supply.

One preliminary design for the CH-53G shows a highly integrated solution weighing below 1% of the helicopter MTOW. It features the complete integration of all mechanical and hydraulic components in the rotating frame. This architecture would remove the need for a hydraulic slip ring, since the pump is driven by the rotor itself and does not need an extra power pickup.

A further simplification of the IBC system could be realized if the design would consider the IBC-specific load / piston travel characteristics. Flight and wind tunnel test data have shown that the average mechanical power consumed by the blade pitch motion is relatively small, because the energy flow is reversed during a considerable part of each rotor revolution. Thus, the power demand of IBC could be drastically reduced if a "regenerative" IBC system was designed that allows for power recovery. One solution, the so-called IBC displacement system, has been tested at ZFL. This system does not rely on the servo valve principle but directly connects a variable displacement pump with specialized actuators. This setup enables the desired bi-directional energy flow between the actuator and the pump. This technical approach can greatly simplify the IBC system layout and may help to introduce IBC into existing or new helicopters.

The experience gained from the previous and the current test campaigns bolsters ZFL's view that IBC is a practical and valuable solution. It can be designed into new helicopters but has also retrofit capability and promises a high benefit-to-cost ratio.

Acknowledgement

The work presented in this paper was primarily funded by the German Federal Office of Defense, Technology, and Procurement (BWB). The authors also like to thank the staff of the German Federal Armed Forces Technical and Airworthiness Center for Aircraft (WTD 61) in Manching for their continuous support of this successful IBC campaign.

References

[1] P. Richter, H.-D. Eisbrecher, V. Klöppel, "Design and First Tests of Individual Blade Control Actuators", 16th European Rotorcraft Forum, 1990.

[2] W. R. Splettstoesser et al., "BVI Impulsive Noise Reduction by Higher Harmonics Pitch Control: Results of a Scaled Model Rotor Experiment in the DNW", 17th European Rotorcraft Forum, Berlin, 1991.

[3] D. Teves, V. Klöppel, P. Richter, "Development of Active Control Technology in the Rotating Frame, Flight Testing and Theoretical Investigations", 18th European Rotorcraft Forum, Avignon, 1992.

[4] S. A. Jacklin, A. Blaas, S. M. Swanson, D. Teves, "Second Test of a Helicopter Individual Blade Control System in the NASA Ames 40-by-80 feet Wind Tunnel", 2nd AHS International Aeromechanics Specialists Conference, 1995.

[5] U.T.P. Arnold, M. Müller, P. Richter, "Theoretical and Experimental Prediction of Individual Blade Control Benefits", 23rd European Rotorcraft Forum, Dresden, 1997.

[6] S.M. Swanson, S.A. Jacklin, A. Blaas, G. Niesl, R. Kube, "Acoustic Results from a Full-Scale Wind Tunnel Test Evaluating Individual Blade Control", 51st AHS Annual Forum, Fort Worth, 1995.

[7] D. Schimke, U. Arnold, R. Kube, "Individual Blade Root Control Demonstration - Evaluation of Recent Flight Tests", 54th AHS Annual Forum, Washington D.C., 1998.

[8] D. Morbitzer, U. Arnold, M. Müller, “Vibration and Noise Reduction through Individual Blade Control Experimental and Theoretical Results”, 24th European Rotorcraft Forum, Marseille, 1998.

[9] O. Kunze, U. Arnold, S. Waaske, “Development and Design of an Individual Blade Control System for the Sikorsky CH-53G Helicopter”, 55th Annual Forum of the American Helicopter Society, Montreal, 1999.

[10] M. Mueller, U. Arnold, D. Morbitzer, “On the Importance and Effectiveness of 2/rev IBC for Noise, Vibration and Pitch Link Load Reduction”, 25th European Rotorcraft Forum, Rome, 1999.

[11] A. Haber, S.A. Jacklin, G. deSimone, “Development, Manufacturing, and Component Testing of an Individual Blade Control System for a UH-60 Helicopter Rotor”, AHS Aerodynamics, Acoustics, and Test and Evaluation Technical Specialists Meeting, San Francisco, 2002.

[12] P. Richter, W. König, „Einzelblattsteuerung (IBC) für den Transporthubschrauber CH-53G“, Deutscher Luft- und Raumfahrtkongress, Hamburg, 2001.

[13] U. Arnold, G. Strecker, “Certification, Ground and Flight Testing of an Experimental IBC System for the CH-53G helicopter”, 58th Annual Forum of the American Helicopter Society, Montreal, 2002.

[14] S.A. Jacklin, A. Haber, G. de Simone, et al., “Wind Tunnel Test of a UH-60 Individual Blade Control System for Adaptive Performance Improvement and Vibration Control“,58th Annual Forum of the American Helicopter Society, Montreal, 2002.

[15] W. Johnson, W., “Self-Tuning Regulators for Multicyclic Control of Helicopter Vibrations”, NASA Technical Paper No. 1996, 1982.

[16] G. Lehmann; R. Kube, “Automatic Vibration Reduction at a Four Bladed Hingeless Model Rotor – A Wind Tunnel Demonstration”, Vertica Vol. 14, No. 1, pp. 69-86, 1990.

[17] T. Millot, W. Welsh, “Helicopter Active Noise and Vibration Reduction”, 25th European Rotorcraft Forum, Rome, 1999.

[18] D.Fürst, T. Auspitzer, M. T. Höfinger, B. G. van der Wall, “Numerical Investigation of Vibration Reduction Through IBC for a 20to Helicopter Rotor Model”, 28th European Rotorcraft Forum, Bristol, 2002.

[19] Ch. Kessler, D. Fürst, U. Arnold, “Open Loop Flight Test Results and Closed Loop Status of the IBC System on the CH-53G Helicopter ”, 59th Annual Forum of the American Helicopter Society, Phoenix, Arizona, 2003.

[20] U. Arnold, “Recent IBC Flight Test Results from the CH-53G Helicopter”, 29th European Rotorcraft Forum, Friedrichshafen, Germany, 2003.

[21] J. Shaw, N. Albion, E.J. Hanker, R.S. Teal, “Higher Harmonic Control: Wind Tunnel Demonstration of Fully Effective Vibratory Hub Force Suppression”, 41st Annual Forum of the American Helicopter Society, Forth Worth, Texas, 1985.

[22] M. Achache, M. Polychroniadis, “Development on an ExperimentalSystem for Active Control of Vibrations on Helicopters – Development Methodologyfor an Airborne System”, Vertica Vol. 11, No. ½, pp. 123-138, 1987.

[23] E.R. Wood, R.W. Powers, J.H. Cline, C.E. Hammond, “On Development and Flight Testing a Higher Harmonic Control System”, ”, 39th Annual Forum of the American Helicopter Society, St. Louis, Mo, 1983.

[24] M. Bebesel, D. Roth, R. Pongratz, “Reduction of BVI Noise on Ground-In-Fight Eevaluation of Closed-Loop Controller”, 28th European Rotorcraft Forum, Bristol, 2002.

[25] D. Fuerst, C. Kessler, et al., „Closed Loop IBC System and Flight Test Results on the CH-53G Helicopter”, 60th Annual Forum of the American Helicopter Society, Baltimore, MD, 2004.

[26] R.P. Cheng, M.B. Tischler, R. Celi, „A High-Order, Time Invariant, Linearized Model for Application to HHC/AFCS Interaction Studies, 59th Annual Forum of the American Helicopter Society, Phoenix, Arizona, 2003.